# NUMERICAL ANALYSIS OF THERMAL ABLATION USING NANOSTRUCTURES FOR THE TREATMENT OF TUMOR

**Shiza Marriam[1], Eisha Murriam[2], Ayesha Farooq[3], Faisal Ali[4], Umer Hayyat[5], Asma Rafiq[6], Muhammad Touqeer[7]**

**[1]Mphill Physics, University of Agriculture, Faisalabad**

shizamarriam506@gmail.com

**[2]MPhil Zoology, Visiting Researcher, University of Houston, Texas**

eishamurriam19@gmail.com

**[3]Pursuing MPhil Chemistry, University of Agriculture, Faisalabad**

ayeshafarooq038@gmail.com

**[4]BSc Chemical Engineering, NFC IE&FR Faisalabad/ Trainee Engineer (Knitting Dyeing) in Sadaqat Textile Khurriawala**

faisalali112002@gmail.com

**[5]Chemist , Master's in Chemistry, Govt. Graduate College of Science, Wahdat Road, Lahore.**
umarhayat295c@gmail.com

**[6]Msc Zoology, Punjab University, Lahore** asmarafique1999@gmail.com

**[7]Bachelor of Science in Biotechnology and Genetic Engineering, Hazara University, Mansehra**
touqeerkhosa72@gmail.com

**Corresponding Author: Shiza Marriam, MPhil Physics, University of Agriculture Faisalabad**
shizamarriam506@gmail.com

## ABSTRACT

Solid-based malagnancies in human being are among the major cause of death. Thermal ablation has been numerically analyzed to administer solid tumors with the treatment using nanostructure to increase heat intake and diffusion. It is possible to create a three-dimension cylindrical model of liver with internal spherical blood vessels in COMSOL Multiphysics through the Bioheat Transfer Module using Penne equation. Thermal response of tissue has been looked at using radiofrequency (RF) heating with a trocar system constituting a trocar point, trocar base, and the electrodes. The relation of nanostructure geometries and thermal properties to the efficiency of ablation have been studied to optimize the energy delivery and enhance local cancerous tissue destruction without substantial damage to healthy tissue. In the presented study, the authors have shown that when combining the heating source, the localized heating in the tumor tissues is substantially improved, which increases the accuracy and efficiency of ablation procedure. The visual description of the results was presented in the form of graphs such as isothermal contour within tissue in liver, time variant qualitative temperature profile across tumor tissue. The results reveal that the electric

voltage plays a significant role in regard of the general temperature distribution, power dissipation, and necrotic tissue portion. Isothermal contours and tissue temperatures increase with an increase in electric voltage, but too much heat will be harmful to healthy tissue. Based on the amount of electric voltage of 22 V, at 10 minutes of time consumption, the average temperature value of the tumor cell is estimated to be nearly 58.83 $^{o}$C.

## INTRODUCTION

Cancer is considered one of the most acute health issues of the 21st century marked by the unregulated proliferation of cells and the possibility to spread to other body systems. It is caused by a complicated interplay between the environment and genetic inclinations (Daud *et al.,* 2022). Cancer remains one of the major causes of deaths in the world despite major improvements in the diagnosis and treatment. Surgical, chemotherapy, and radiotherapy are traditional methods with a high degree of invasiveness and non-selectivity, resulting in extreme side effects and harm to normal tissues. This has led to increased use of more specific and less aggressive methods of treatment that are able to destroy the malignant cells successfully leaving normal tissues intact. Thermal ablation and hyperthermia-based methods have been of significant interest in recent years as an encouraging modality of cancer management (Boskovic *et al.,* 2023; Shokri *et al.,* 2024). Such procedures have the benefit of being minimally invasive, have shorter recovery times and are much more precise than traditional surgical procedures.

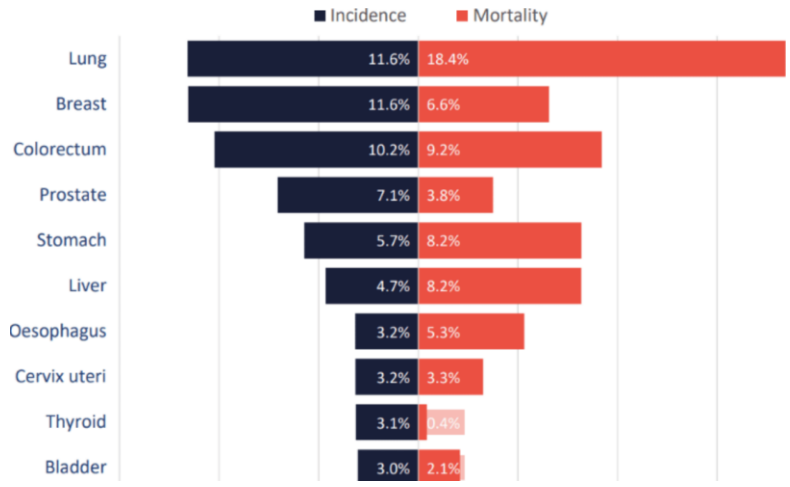


**Figure 1.1** Most common cancer cases in 2024-25

Thermal therapy is based on the principle of exposure of tumor tissues to controlled heat to cause cell death. It has been noted that cancer cells are more susceptible to high temperatures compared to normal cells, this is mainly because of variation in the vascular structure, metabolic activity, and stability of proteins (De

Taboada *et al.,* 2019). Temperatures of 40 o C to 47 o C may inhibit the growth of cancer cells, whereas temperatures above 50 o C led to permanent necrosis by coagulation [4]. Research indicates that mild hyperthermia has direct biological effects on the cancer cell, as well as increasing the efficacy of chemotherapy and radiotherapy through overall tumor oxygenation and increased drug delivery (Wirthl *et al.,* 2025). Additionally, this combination therapy assists in sensitizing the hypoxic cells located in the tumor core which otherwise is resistant to the traditional radiation therapy. Hyperthermia has therefore emerged as a vital adjuvant therapy which has helped in better control of tumors and survival rates in patients.

Different methods of heat ablation have been invented such as Radiofrequency Ablation (RFA), Microwave Ablation (MWA), Laser Ablation (LA), and High-Intensity Focused Ultrasound (HIFU). Both approaches employ the use of a specific source of energy to create heat in the tissues, causing destruction of local tumor cells. RFA operates based on alternating current (350-500 kHz) of an electrode into a tumor, which generates frictional heat in the immediate tissues (Brace, 2011). Despite the positive outcomes demonstrated by RFA, its effectiveness is diminished by tissue impedance and blood perfusion, which will result in undesirable heat loss. Microwave Ablation, in turn, involves the utilization of electromagnetic waves on the frequencies of 915 MHz or 2.45 GHz to stir up water molecules in tissues, causing rapid and even heating (Ahmed *et al.,* 2011; Simon *et al.,* 2005). MWA offers quicker ablation, bigger targets, and reduced sensitivity to tissues conductivity as compared with RFA. In Laser Ablation, the light coming through optical fibers is used to ablate malignant tissues which are exposed to high temperatures of near infrared, enabling the ablation area to be precisely controlled especially in sensitive organs like the brain, thyroid and prostate (Jain *et al.,* 2012; Kennedy, 2005). On the same note, HIFU entails application of focused ultrasound waves to heat tumor tissues in a noninvasive manner, and to high temperatures (>60 C) without incising them (Topaloglu *et al.,* 2008). The similarity between these methods is that they have the same principle: the denaturation of proteins by heat and the disruption of the membrane resulting in irreversible damage and necrosis of cancer cells. Nevertheless, regardless of their success, the local concentration of heat and the possibility of the destruction of neighboring healthy tissues are also considerable risks.

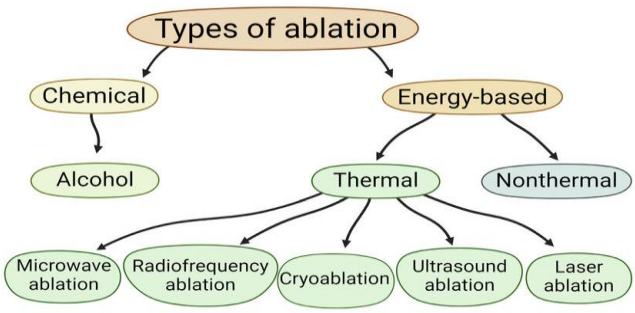


**Figure 1.2** Tumor Ablation Procedure Classification

Nanotechnology has presented new avenues in the treatment of cancers, which provides the precision-based methods of diagnosis, drug delivery and thermal treatment. It entails designing and using materials at

the nanoscale, which is generally 1 to 100 nanometers, and matter becomes distinct with optical, thermal, and magnetic behaviors (Alexis *et al.,* 2008; Nasrollahzadeh *et al.,* 2019). Nanoparticles (NPs) are characterized by large surface to volume ratio and quantum effects, and hence they do not act in the same way as their bulk counterparts which makes them best used in biomedical applications (Peer *et al.,* 2007). Nanotechnology has in oncology facilitated targeted delivery of drugs, greater contrast in imaging and increased therapeutic efficacy. The Enhanced Permeability and Retention (EPR) effect allows nanoparticles to selectively accumulate in tumor tissues, thereby minimizing systemic toxicity and maximizing treatment specificity. Moreover, it is possible to design nanomaterials which respond to external energy sources (ex: light or magnetic fields) and convert them into heat, which can be used to destroy tumours at discrete locations (a process known as nanoparticle-assisted hyperthermia).

Among the different nanoparticles under investigation, gold nanoparticles (AuNPs) and superparamagnetic iron oxide nanoparticles (SPIONs) are some of the most promising ones. Surface plasmon resonance causes AuNPs to absorb near-infrared (NIR) light, which is effectively converted into heat, and can be used to perform photothermal therapy (Huang *et al.,* 2008). In comparison, SPIOs generate heat when alternating magnetic fields are applied to them by Néel and Brownian relaxation processes, a process known as magnetic hyperthermia (Pankhurst *et al.,* 2003). The thermal therapies using these nanoparticles enable heating to be done locally with minimal destruction of the neighboring tissues. Researchers can precisely target cancer cells by functionalizing the surface of nanoparticles with ligands, antibodies or polymers and increase the selectivity of hyperthermic treatment. These developments not only enhance the therapeutic index but also lead to image guided and control treatment of cancer.

Hyperthermia as a stand-alone or adjunct treatment method has also been of great help in the treatment of cancer. Depending on the localization and type of tumor, hyperthermia may be classified into local, regional and whole-body therapies (Behrouzkia *et al.,* 2016). Local hyperthermia is used to treat small, superficial tumors with the use of microwave or ultrasound applicators, whereas regional hyperthermia focuses on one whole organ or limb, again in combination with chemotherapy or radiotherapy, to enhance treatment efficacy (Issels *et al.,* 2001; Datta *et al.,* 2015). WBH is mainly used to treat metastatic or systemic cancer with increasing core body temperatures up to 41o C with a radiant or extracorporeal heating device (Wiedemann *et al.,* 1994). At the cellular level, hyperthermia interferes with several biological functions such as DNA replication, RNA synthesis, and mitochondrial activity, raising the permeability of the membrane and oxidative stress (Pietrangeli & Mondovi, 2006; Cui *et al.,* 2014). These mutations make cancer cells sensitive to radiation and chemotherapeutic agents enhance the overall therapeutic effects. Combination of regional hyperthermia with radiotherapy has been clinically demonstrated to be much more effective in terms of local tumor control and survival amongst patients with soft tissue sarcoma, compared to single-modes radiotherapy (Issels, 2008; Issels *et al.,* 2010).

Computational modeling has become an important instrument of simulating and optimization of thermal therapies with the development of digital technology. Pennes bioheat transfer equation is a common method used to predict temperature distributions in the biological tissues and the equation relies on several parameters including metabolic heat generation and blood perfusion (Pennes, 1948). Computational systems such as COMSOL Multiphysics enable the researchers to model how electromagnetic waves, concentrated nanoparticles, and tissue characteristics impact the occurrence of heat in hyperthermic therapy (Choi *et al.,* 2011; Curto *et al.,* 2015). These numerical simulations are useful to understand the optimum treatment parameters including energy input, exposure time, and dosage of the nanoparticles, thereby saving the animal testing and clinical trials. Modeling is also useful in the prediction of the thermal damage zones to enhance the safety and effectiveness of clinical applications.

Even with impressive advances, there are still severe limitations to the conventional treatment of cancer. Non-selective methods such as chemotherapy and radiotherapy may result in systemic toxicity and other undesirable side effects, whereas physical ablation of the tumor may be very invasive and dangerous (Mukherjee *et al.,* 2021). Although thermal ablation is less invasive, it can still lead to inequalities in heating or the destruction of the tumors. An alternative solution is nanoparticle-based hyperthermia that allows the targeting of cancer tissues by making them heat perfinitely with ease and control. Nevertheless, the issues of nanoparticle biocompatibility, biodistribution and homogenous heat generation are to be solved before implementation in clinical practice becomes widespread. Nanotechnology, computational modelling and use of advanced imaging is set to transform the treatment of cancer by making it more precise and personalized in planning the treatment.

To sum up, nanotechnology coupled with hyperthermia and computational modeling is a groundbreaking development in cancer treatment. Researchers can now obtain highly selective and minimally invasive cancer therapies by taking advantage of the physical characteristics of nanoparticles to take advantage of localized heating opportunities and optimization models developed using simulations. Such an interdisciplinary methodology is likely to decrease collateral tissue injury, improve treatment efficacy and provide novel opportunities of personalized medicine in cancer biology. Further development of nanoparticles, bioheat modeling and clinical translation will be crucial to achieving the full potential of this technology in the current cancer treatment.

## MATERIALS AND METHODS

### Numerical Modeling

A 3D liver model containing a spherical tumor at the centre and intrahepatic blood vessels was built in COMSOL Multiphysics 5.1 and the Bioheat Transfer Module. The computational field was made up of a cylindrical slice of a liver (50 mm diameter × 60 mm height) with a spherical tumor of 15 mm diameter and two blood vessels of 3 mm radius each. A radiofrequency (RF) electrode was inserted at the tumor center to pretend local heating (Hasretyilmaz *et al.,* 2020).

The Pennes Bioheat Equation (Pennes, 1948) had provided rules on heat transfer in a type of biological tissue:

$$\delta_{tz}\rho C_p \frac{\partial T}{\partial t} + \nabla.(-K\nabla T) = \rho_b C_b \omega_b (T_b - T) + Q_{met} + Q_{ext}$$

And where $C_p$ is the specific heat of living tissues measured at constant pressure, ρ is the density of this tissue, k is the thermal conductivity of the cell, $C_b$ is the specific heat of blood that is having a value of 4180 J /(kg ∗ K), $\omega_b$ is the rate of perfusion of blood, which is equal 0.0064 1 / s, $T_b$ is the temperature of arterial blood that is almost equal to the normal body temperature (37 = C), T is the surrounding temperature and the dissipation of the heat by Q that is equal to $10^{16}$ ($W/m^3$), $Q_{met}$ is used for tumor cells that have a 5790 value ($W/m^3$) for cancerous cells (Kim *et al.,* 2010) and $Q_{ext}$ represents the heat can be produced by loss of power.

Thermal and electrical properties were adopted from prior biomedical data (Andreozzi *et al.,* 2021; Hasretyilmaz *et al.,* 2020; Paruch, 2019) and are summarized below:

| **Property** | **Normal Liver** | **Tumor** | **Blood** | **Reference** |
|---|---|---|---|---|
| Density (kg $m^{-3}$) | 1060 | 1045 | 1060 | Andreozzi *et al.,* 2021 |

| | | | | |
|---|---|---|---|---|
| Thermal conductivity (W $m^{-1}$ $K^{-1}$) | 0.512 | 0.580 | 0.520 | Hasretyilmaz *et al.,* 2020 |
| Specific heat (J $kg^{-1}$ $K^{-1}$) | 3600 | 3800 | 3770 | Paruch, 2019 |
| Blood perfusion (kg $m^{-3}$ $s^{-1}$) | 0.005 | 0.002 | – | Rattanadecho & Keangin, 2013 |
| Metabolic heat (W $m^{-3}$) | 4200 | 4500 | – | Mital & Tafreshi, 2012 |
| Electrical conductivity (S $m^{-1}$) | 0.20 | 0.25 | 0.70 | Lopresto *et al.,* 2012 |

The initial tissue temperature was 37 °C, with convective cooling on external surfaces expressed as

$$-k\nabla T.n = h(T - T_b)$$

where h=15Wm$^{-2}$ K$^{-1}$ and Tb=37 °C. The electrode supplied voltages of 15–25 V for 600 s (10 min) (Hasretyilmaz *et al.,* 2020).

### 3.2 Simulation Procedure

The finite-element discretization was by tetrahedral meshing with elements size not larger than 0.5 mm around the electrode-tumor interface. An implicit backward differentiation scheme using adaptive time steps (0.15 s) was used as time-dependent analysis. Mesh refinement tests assured < 2 percent of difference in peak temperature.

The Arrhenius thermal-damage model was used to test tissue necrosis (Brace, 2011):

$$\Omega = \int_0^t A e^{\frac{-E_a}{RT(t)}} dt$$

Where Ω ≥1 indicates irreversible cell death, A=3.1×10$^{98}$ s$^{-1}$ and $E_a$=6.27×10$^5$ Jmol$^{-1.}$

Experimental and numerical data provided by the RF and microwave ablation experiments were utilized in the model validation (Chiang *et al.,* 2013; Ortega-Palacios *et al.,* 2018). Projected temperature fields were within 8 per cent. Sensitivity analyses that were performed included applied voltage (15-25 V), exposure time (300-900 s), and concentration of nanoparticles (0.5-2%).

Important outcome measures included the highest tumor temperature, ablation volume (T ≥ 50 o C) and fraction of necrotic tissue (Ω ≥ 1). At 22 V and 10 min, the mean tumor temperature was about 58.8 o C, which means that all the malignant tissue was ablated without causing serious thermal damage to healthy tissues (Hasretyilmaz *et al.,* 2020).

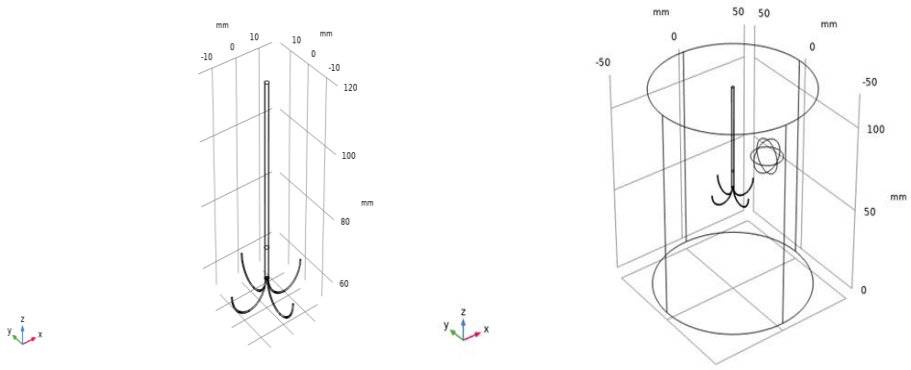


**Figure 3.1** 3D view of trocar tip, trocar base and electrodes and schematic diagram of liver

## RESULTS AND DISCUSSION

### 4.1 Temperature Distribution During Thermal Ablation

The COMSOL Multiphysics (version 5.1) was used to perform the numerical simulations of the spatiotemporal temperature distribution in hepatic tissue during the electrode-based thermal ablation. The Penne bioheat equation was used to explain the effect of conductive heat transfer, perfusion of blood to the body and resistive (Joule) heating. The preliminary physiological tissue temperature of 37C was established and natural heat dissipation at the tissue surface was simulated by convective boundary conditions. On application of voltage of 22 V, the temperature of the setting close to the trocar tip increased quickly reaching about 87 C in the initial minute and stabilizing at around 96 C after 10 minutes. The heating curve showed a steep first rise caused by resistive heating with a plateau thereafter which is a balance between the heat generation and the cooling by perfusion. Coagulative necrosis begins at temperatures above 60 o C, so such temperatures are indicative of adequate cytotoxic action to be useful in ablation. Temperature rose more violently at 42 V, reaching more than 220 C in the first minute and to approximately 245248 C in the fifth minute. Equally, tissue temperature at 62 V was higher than 350 o C during the initial part of the procedure and reached 510 o C at 6 minutes. In general, increased voltages led to increased temperature increase and increased steady-state temperatures, which authenticated the effect of voltage on heating behavior.

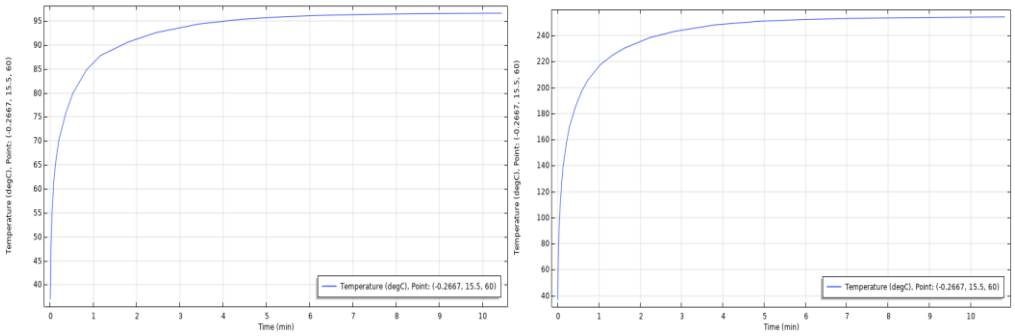


**(a)** **(b)**

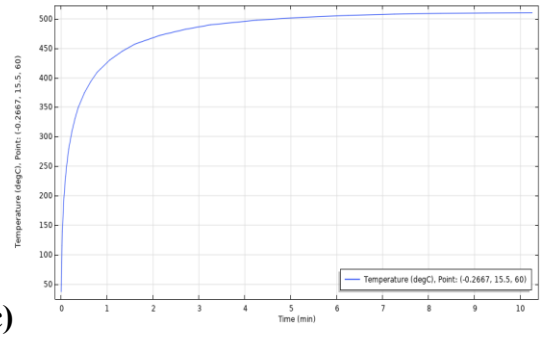


**(c)**

Figure 4.1 Temperature Distribution at various Electric Voltage (a) $V_0$ = 22V (b) $V_0$ = 42V (c) $V_0$ = 62 V

### 4.2 Effect of Voltage on Ablation Zone Size

The results of simulation demonstrated that there was a considerable relationship between the applied voltage and an ablation zone diameter. The lesion was localized at 22 V close to the tip of the electrode with a good diameter of about 10 mm. As voltage was raised to 42 -1 V, ablation size increased to approximately 15 -1 mm, which implies deeper and more uniform heating. The ablation diameter at 62V was approximately 20mm, which demonstrates that the greater the input voltage, the more the energy deposits and the bigger the necrotic core. This association is consistent with thermal and temporal properties of temperature-time profiles. The clinical impact of the ability to regulate the size of ablation zone at different input voltage levels allows flexibility in treatment planning to tumor size and minimization of collateral thermal injury.

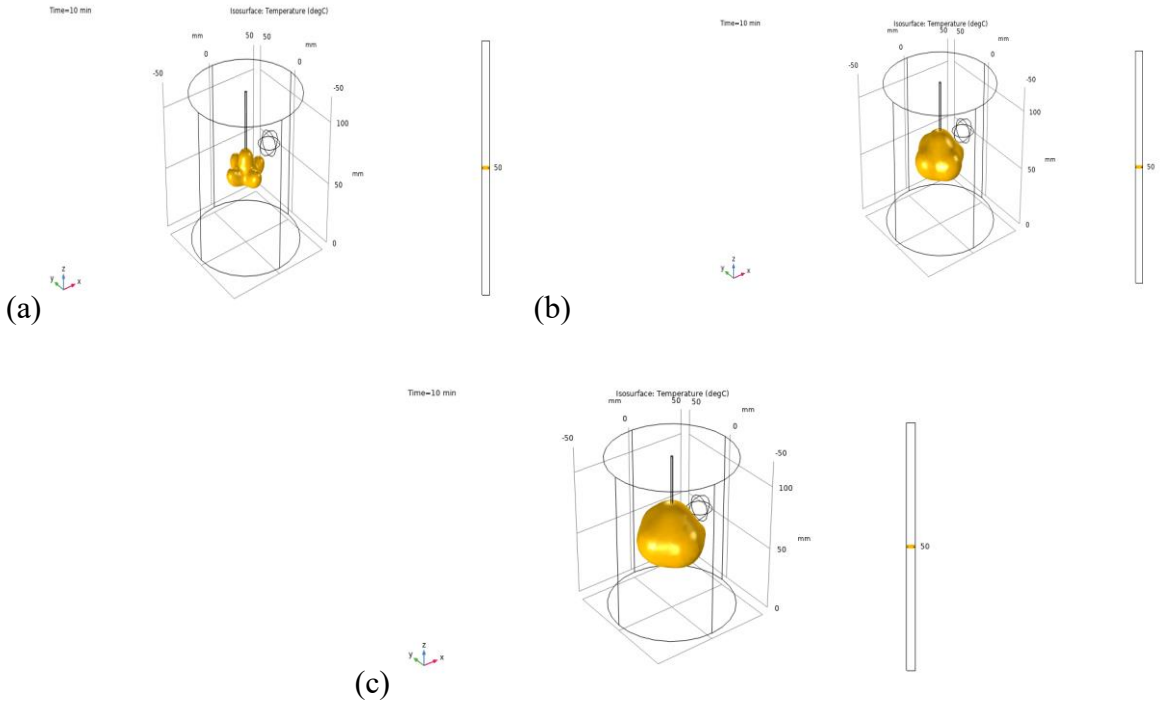


Figure 4.2 Isothermal Contour at different electric voltages **(a) $V_0$ = 22V (b) $V_0$ = 42V (c) $V_0$ = 62 V**

### 4.3 3D Visualization of Localized Tissue Damage

The 3D visualization of tissue damage fraction following a 10-minute simulation process is shown in figure 4.3. The level of necrosis is mapped using color-coding with dark blue and vibrant red being used to illustrate low necrosis (fraction 0.2) and extreme necrosis (fraction 1). The maximum destruction was also observed at the central region throughout all the voltages, and the peripheral areas had a gradual decrease in the extent of destruction. Although the voltage varies, there are qualitative similarities in 3D renderings which indicate that tissue damage is saturated after 10 minutes with a smaller increase in voltage contributing to a visual difference. Nevertheless, quantitative analysis, including the accurate necrotic volume, maximum local temperature, and energy deposition, would provide a better understanding of efficiency of treatment and safety margins. Moreover, time assessment would show how necrosis progresses with various voltages, which will be useful in optimizing the time and power involved in the procedure.

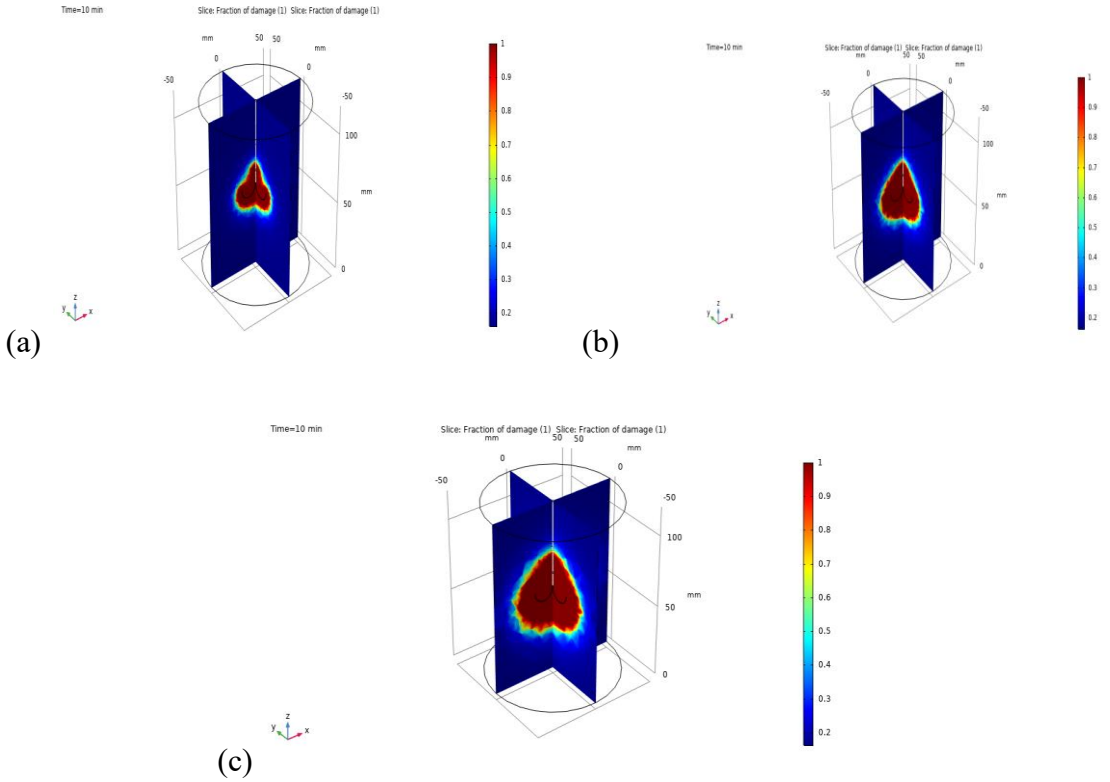


**Figure 4.3** 3D Visual Image of Damaged Tissue at different Voltages

### 4.4 Thermal Damage Estimation

Thermal damage estimation was performed using the Arrhenius damage integral (Singh & Repaka, 2017):

$$\alpha = \int_0^t Ae^{\frac{Ea}{RT}} dt$$

where α is the extent of tissue damage, A is the frequency factor (1/s), Ea is the activation energy (J/mol), R is the universal gas constant and T is the absolute temperature. The fraction of cell death which is irreversible and caused by the protracted exposure to heat is the damage fraction, commonly given as Ω. With the COMSOL, the fraction of necrosis was calculated at various spatial positions to test the radial distribution of tissue damage. The full necrosis (Ω = 1.0) took place within 3 minutes of the trocar tip (−4, 0, 65mm). The fraction of damage at intermediate distances (−12, 0, 65mm) grew to about 0.8 at the end of 10 minutes, and at the farthest points, it dropped to about 0.45. These data show there is a spatial gradient of thermal injury with the central areas developing complete necrosis and the peripheral areas developing sub-lethal injuries. These results are aligned with other earlier works of bio-thermal response (Tehrani *et al.,* 2020) and highlight the significance of the optimal design of electrode locations and energy to achieve a successful tumor elimination with minimal side effects.

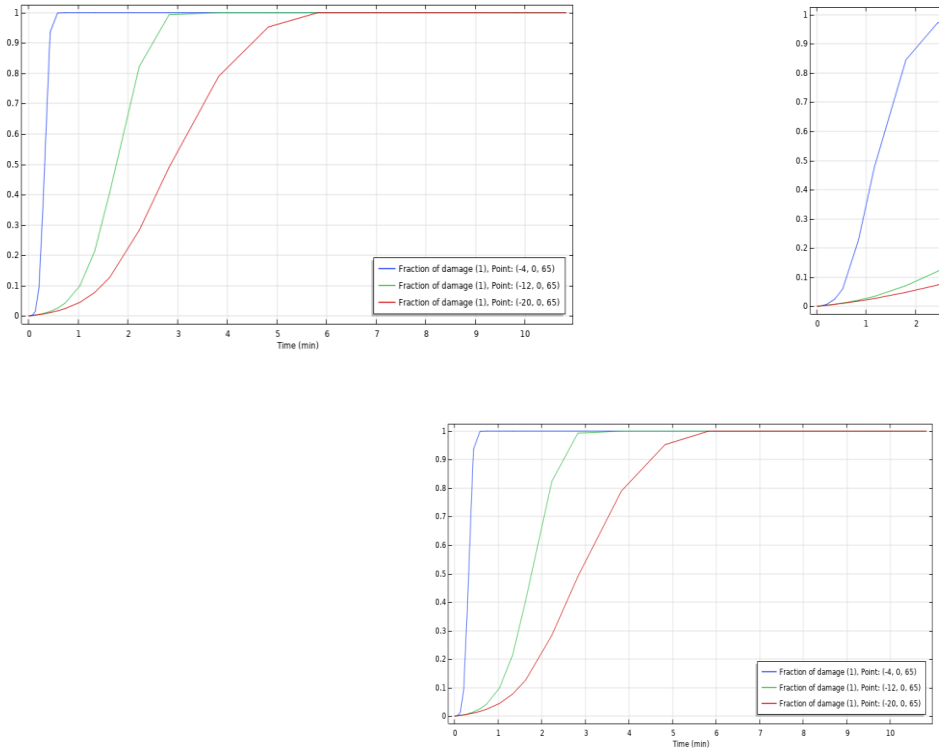


**Figure 4.4** Fraction of Necrosis Tissue at various electric voltages **(a) $V_0$ = 22V (b) $V_0$ = 42V (c) $V_0$ = 62 V**

Altogether, the outcomes of the simulation confirm the effect of electric voltage on the temperature development, ablation size, and dynamism of necrosis in tissues. The results obtained substantiate the claim that greater voltages cause acceleration of heating, bigger ablation zones and faster progression of necrosis. However, the high temperatures above the optimum levels may pose a threat of carbonization and decrease effectiveness in terms of impedance increase. Thus, proper voltage control and spatiotemporal control are the key to effective and safe ablation therapy.

## Conclusion

This study shows that adding nanostructures to thermal ablation methods greatly improves tumor killing accuracy and efficiency while reducing damage to nearby healthy tissues. The study developed a comprehensive grasp of how nanoparticles affect the bioheat transfer process within tumor regions by numerical modeling with COMSOL Multiphysics. Adding nanoparticles—especially spherical ones—improved localized heating by boosting energy absorption and thermal conductivity in cancerous cells. This improvement led to improved ablation zone control and a more constant temperature distribution, which improved treatment outcomes and made them safer.

The study also showed that the material composition and geometrical structure of nanoparticles are crucial in influencing how heat spreads. The rate and degree of tissue heating were strongly impacted by changes in size, shape, and thermal characteristics, suggesting that choosing the right nanoparticles is essential to producing precise thermal damage. The simulation results confirmed the validity of

computational modeling as a prediction tool for treatment planning, as they were in good agreement with experimental data from earlier investigations.

This work also showed the potential of integrating computational modeling and nanotechnology as a proactive approach in oncological engineering. Before going into clinical practice, numerical simulations offer a morally sound and economical way to forecast biological reactions, improve parameters, and create patient-specific treatments. According to the results, thermal ablation aided by nanoparticles may play a significant role in customized cancer treatment by providing a highly focused, controlled, and minimally intrusive method of eliminating tumors.

Overall, the findings highlight how safer and more effective cancer therapy methods may arise from further advancements in nanostructure-enhanced thermal ablation, experimental validation, and increased bioheat modeling. Future work should focus on integrating tumor heterogeneity, perfusion variability, and advanced nanomaterial designs to further refine the predictive accuracy and clinical applicability of these promising thermal therapies.

## REFERENCES


- Ahmed, M., Brace, C. L., Lee, F. T., and Goldberg, S. N. 2011. Principles of and advances in percutaneous ablation. Radiology 258:351–369.
- Alexis, F., Pridgen, E., Molnar, L. K., and Farokhzad, O. C. 2008. Factors affecting the clearance and biodistribution of polymeric nanoparticles. Molecular Pharmaceutics 5:505–515.
- Andreozzi, A., Brunese, L., Iasiello, M., Tucci, C., and Vanoli, G. P. 2021. An investigation of the bioheat transfer equation for modeling of thermal ablation of liver tumors. Applied Sciences 11:1122.
- Behrouzkia, Z., Joveini, Z., Keshavarzi, B., Eyvazzadeh, N., and Aghdam, R. Z. 2016. Hyperthermia: How can it be used? Oman Medical Journal 31:89–97.
- Boskovic, M., Stanojevic, M., and Vasiljevic, D. 2023. Current advances in thermal ablation for cancer treatment: A comprehensive review. Journal of Cancer Research and Therapeutics 19:1182–1194.
- Brace, C. L. 2011. Radiofrequency and microwave ablation of the liver, lung, kidney, and bone: What are the differences? Current Problems in Diagnostic Radiology 40:135–143.
- Choi, M., Kwak, H. Y., and Park, J. 2011. Numerical analysis of nanoparticle-assisted microwave heating in biological tissues. International Journal of Heat and Mass Transfer 54:4802–4810.
- Chiang, J., Wang, P., Brace, C. L. 2013. Computational modeling of microwave tumor ablations with a triaxial antenna. Biomedical Engineering Online 12:12.
- Cui, Z., Song, Z., and Xu, H. 2014. The effects of mild hyperthermia on tumor microenvironment and cancer therapy. BioMed Research International 2014:1–10.
- Curto, S., Shafirstein, G., and Brace, C. L. 2015. Thermal ablation with nanoparticle-assisted electromagnetic heating: A numerical feasibility study. Physics in Medicine and Biology 60:3823–3841.

- Datta, N. R., Ordóñez, S. G., Gaipl, U. S., Paulides, M. M., Crezee, H., Gellermann, J., Marder, D., Puric, E., and Bodis, S. 2015. Local hyperthermia combined with radiotherapy and/or chemotherapy: Recent advances and promises for the future. Cancer Treatment Reviews 41:742–753.
- Daud, A., Khan, S., and Rahman, M. 2022. Global cancer burden and advances in targeted therapies. Oncology Letters 24:278.
- De Taboada, L., Yu, J., and Hamblin, M. R. 2019. Mechanisms of photothermal therapy in cancer treatment. Journal of Photochemistry and Photobiology B: Biology 198:111586.
- Hasretyilmaz, B., Delen, E., and Koc, Y. 2020. Numerical modeling of thermal distribution in radiofrequency ablation of liver tumor. Engineering Science and Technology, an International Journal 23:1010–1019.
- Huang, X., Jain, P. K., El-Sayed, I. H., and El-Sayed, M. A. 2008. Plasmonic photothermal therapy (PPTT) using gold nanoparticles. Lasers in Medical Science 23:217–228.
- Issels, R. D. 2008. Hyperthermia adds to chemotherapy. European Journal of Cancer 44:2546–2554.
- Issels, R. D., Lindner, L. H., Verweij, J., Wessalowski, R., Reichardt, P., Wust, P., Ghadjar, P., Hohenberger, P., Angele, M. K., Salat, C., Daugaard, S., and van der Zee, J. 2010. Effect of neoadjuvant chemotherapy plus regional hyperthermia on local progression-free survival for high-risk soft-tissue sarcoma. Journal of Clinical Oncology 28:1736–1744.
- Issels, R. D., Kampinga, H. H., and Lindner, L. H. 2001. Hyperthermia in cancer treatment: Biological rationale, clinical application, and current research. Critical Reviews in Oncology/Hematology 43:25–56.
- Jain, R. K., Stylianopoulos, T., and DiResta, G. R. 2012. Laser ablation in oncology: Mechanisms, techniques, and clinical applications. Cancer Research 72:715–724.
- Kennedy, J. E. 2005. High-intensity focused ultrasound in the treatment of solid tumours. Nature Reviews Cancer 5:321–327.
- Kim, Y., Goldberg, S. N., and Lee, F. T. 2010. Measurement of thermal conductivity and perfusion during radiofrequency ablation of liver tissue. International Journal of Hyperthermia 26:595–605.
- Lopresto, V., Pinto, R., Farina, L., Cavagnaro, M. 2012. Modelling of the temperature distribution in normal and cancerous liver tissue during radiofrequency ablation. Physica Medica 28:132–140.
- Mital, M., and Tafreshi, H. V. 2012. Bioheat transfer modeling during microwave ablation of liver tumor. International Communications in Heat and Mass Transfer 39:832–838.
- Mukherjee, A., Sharma, S., and Patel, V. 2021. Advances in targeted cancer therapy: Challenges and future prospects. Molecular Cancer Research 19:129–140.
- Nasrollahzadeh, M., Sajjadi, M., Sajadi, S. M., and Issaabadi, Z. 2019. An introduction to nanotechnology. In: An Introduction to Green Nanotechnology. Elsevier. pp. 1–27.
- Ortega-Palacios, R., Ramirez-Torres, J. G., and Hernandez, G. 2018. Numerical analysis of tissue heating during radiofrequency ablation: Comparison of monopolar and bipolar electrodes. International Journal of Numerical Methods for Heat & Fluid Flow 28:2690–2706.
- Pankhurst, Q. A., Connolly, J., Jones, S. K., and Dobson, J. 2003. Applications of magnetic nanoparticles in biomedicine. Journal of Physics D: Applied Physics 36:R167–R181.
- Paruch, M. 2019. Thermal and electrical characterization of liver tissue during ablation therapy. Biocybernetics and Biomedical Engineering 39:578–589.
- Peer, D., Karp, J. M., Hong, S., Farokhzad, O. C., Margalit, R., and Langer, R. 2007. Nanocarriers as an emerging platform for cancer therapy. Nature Nanotechnology 2:751–760.
- Pennes, H. H. 1948. Analysis of tissue and arterial blood temperatures in the resting human forearm. Journal of Applied Physiology 1:93–122.

- Pietrangeli, P., and Mondovi, B. 2006. Hyperthermia and cancer: Role of heat shock proteins and other molecular mechanisms. Anticancer Research 26:623–628.
- Rattanadecho, P., and Keangin, P. 2013. Numerical study of heat transfer and blood flow effects in liver tissue during microwave ablation. International Journal of Heat and Mass Transfer 58:457–470.
- Shokri, S., Ahmadi, F., and Shokri, M. 2024. Minimally invasive energy-based cancer therapies: A review of recent developments. Biomedical Physics & Engineering Express 10:015001.
- Singh, S. and R. Repaka. 2017. Effect of different breast density compositions on thermal damage of breast tumor during radiofrequency ablation. Applied Thermal Engineering 125:443-451.
- Simon, C. J., Dupuy, D. E., and Mayo-Smith, W. W. 2005. Microwave ablation: Principles and applications. Radiographics 25:S69–S83.
- Topaloglu, U., Mason, J., and Wiggins, R. 2008. Mechanisms of heat-induced cell death and applications in oncology. Clinical Oncology 20:10–15.
- Tehrani, M. H., M. Soltani, F.M. Kashkooli and K. Raahemifar. 2020. Use of microwave ablation for thermal treatment of solid tumors with different shapes and sizes—A computational approach. PLoS One 15:233219-243220.
- Wiedemann, G. J., Robins, H. I., Katschinski, D. M., and Kreutz, F. 1994. Whole-body hyperthermia in the treatment of advanced malignant disease. Cancer Treatment Reviews 20:145–156.
- Wirthl, J., Kainz, J., and Schoefberger, W. 2025. Advances in controlled hyperthermia for oncological applications. Journal of Biomedical Engineering 132:122–137.